Composite Structures **22** (1992) 47–57

Buckling of polar and rectilinearly orthotropic annuli under uniform internal or external pressure loading

Lei Fu & Anthony M. Waas

Department of Aerospace Engineering, College of Engineering, University of Michigan, Ann Arbor, Michigan 48109-2140, USA

The problem of the out of plane buckling of polar orthotropic annuli under uniform internal or external pressure loading has been investigated with the assumption of axisymmetry by numerous researchers. In this paper, the buckling of polar and rectilinearly orthotropic annuli subjected to internal or external pressure loading is examined without restriction to axisymmetric buckling modes. The buckling analyses are performed in both the polar orthotropic and rectilinearly orthotropic cases by the Rayleigh–Ritz method. In the rectilinearly orthotropic cases, the pre-buckling solution is obtained via Galerkin's method as no known exact solution exists, while in the polar orthotropic case the pre-buckling stress distributions used are exact. It is found in both the polar orthotropic and the rectilinearly orthotropic annuli that restriction to axisymmetric buckling modes in the externally pressurized case does not produce the lowest buckling load over a significant range of annuli aspect ratios. Example results for commercially used fiber/matrix systems are presented and discussed, and it is concluded that the unwarranted assumption of axisymmetry actually produces nonminimum buckling loads.

NOTATION

c	$R_{\text{inner}}/R_{\text{outer}}$
D_r	$E_r h^3/12(1-\nu_r\nu_\theta)$
D_θ	$E_\theta h^3/12(1-\nu_r\nu_\theta)$
$D_{r\theta}$	$G_{r\theta}h^3/12$
D_1	$\nu_r D_\theta$ or $\nu_\theta D_r$
E_r, E_θ	Young's modulus in the radial and circumferential directions
$G_{r\theta}$	Shear modulus in the r, θ plane
h	Thickness of plate
k	$(D_\theta/D_r)^{1/2}$
M_{Gal}	Number of terms in series associated with Galerkin's Method
N_{Ritz}	Number of terms in series associated with the Rayleigh–Ritz Method
p	Uniform in-plane pressure at the inner edge ($r = R_{\text{inner}}$)
q	Uniform in-plane pressure at the outer edge ($r = R_{\text{outer}}$)
r, θ	Polar coordinates of a point in the mid-plane of the annular plate
$R_{\text{inner}}, R_{\text{outer}}$	Radii of inner and outer edges, respectively
T	Potential energy due to in-plane forces during bending
V	Strain energy
$w(r, \theta)$	Lateral out-of-plane displacement as a function of r and θ
α	Angle between principal material axes and x, y axes
λ	Wave number
ν_r, ν_θ	Poisson's ratios
Π	Total potential energy, $\Pi = V + T$
$\Phi_{m,r\theta}$	$\dfrac{\partial \Phi_m}{\partial r\,\partial\theta}$

1 INTRODUCTION

Fibrous composite materials continue to be an attractive alternative candidate for construction

Composite Structures 0263-8223/92/$05·00

purposes. Thin plate and shell type structures are widely used in the Aerospace Industry as load bearing structural elements. Consequently, their response and stability constitute topics of interest to the design engineer.

Buckling of a load bearing structural element is an undesirable phenomenon. Because of this, many analyses have been reported in the open literature dealing with the stability of composite structures. The buckling of circular polar orthotropic plates[1,2] and numerous other publications on the buckling of polar orthotropic annular plates[3-6] have appeared in the literature. In these studies, the buckling mode shape has been assumed to be axisymmetric. Consequently, the possibility of a nonaxisymmetric buckling mode has not been investigated. It had been shown[7] that nonaxisymmetric buckling modes exist for polar orthotropic circular plates. Motivated by this, the buckling problem for polar orthotropic and rectilinearly orthotropic annuli is studied here in more general terms where no restrictions such as axisymmetry are placed upon the buckling mode.

The pre-buckling stress states of the polar orthotropic annuli are obtained in closed form, as was shown previously in Ref. 8. As no exact solution for the pre-buckling stress state of the rectilinearly orthotropic annuli exists in the present literature, the stress states are obtained approximately utilizing the Galerkin method.[9] The Rayleigh-Ritz method is used in both the polar orthotropic and the rectilinearly orthotropic cases for the buckling analysis. The effect of the aspect ratio on the association of the lowest buckling load with axisymmetric or nonaxisymmetric buckling mode is examined.

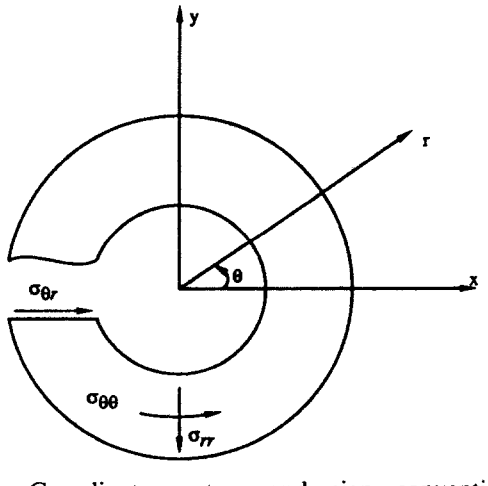

Fig. 1a. Coordinate system and sign convention for annulus.

Previously, this analysis was performed in conjunction with the Rayleigh-Ritz method where the buckling mode was assumed to be axisymmetric.[3,10] In our formulation of the polar orthotropic and rectilinearly orthotropic annulus, we remove the restriction to axisymmetry by allowing variations in the circumferential variable, θ, to take into account nonaxisymmetric buckling of the annuli.

The formulation used in the polar orthotropic case was specialized to the case of isotropy (by using appropriate simplifications to the material properties) and the resulting data were found to agree well with previously published results reported in Ref. 12.

2 PROBLEM FORMULATION

2.1 Polar orthotropic annulus

We consider a thin annular plate of uniform thickness h, subjected to uniform inplane edge pressure loading (external or internal). The material of the plate is assumed to be homogeneous and linearly elastic, exhibiting polar orthotropy.

Assuming a state of generalized plane stress and with reference to Fig. 1a, the pre-buckling stresses are given by[8]:

$$\sigma_{rr}=\frac{pc^{k+1}-q}{1-c^{2k}}\left(\frac{r}{R_{\text{outer}}}\right)^{k-1}$$

$$-\frac{p-qc^{k-1}}{1-c^{2k}}c^{k+1}\left(\frac{R_{\text{outer}}}{r}\right)^{k+1}$$

$$\sigma_{\theta\theta}=\frac{pc^{k+1}-q}{1-c^{2k}}k\left(\frac{r}{R_{\text{outer}}}\right)^{k-1}$$

$$+\frac{p-qc^{k-1}}{1-c^{2k}}kc^{k+1}\left(\frac{R_{\text{outer}}}{r}\right)^{k+1} \tag{1}$$

$$\sigma_{r\theta}=0$$

where a positive sign is associated with a compressive stress component.

The strain energy, V, of bending and the potential energy due to the mid-plane forces, T, are given by:[10]

$$V=\frac{1}{2}\int_0^{2\pi}\int_{R_{inner}}^{R_{outer}}\left[D_r\left(\frac{\partial^2 w}{\partial r^2}\right)^2 + 2D_1\left(\frac{\partial^2 w}{\partial r^2}\right)\left(\frac{1}{r}\frac{\partial w}{\partial r}+\frac{1}{r^2}\frac{\partial^2 w}{\partial \theta^2}\right) + D_\theta\left(\frac{1}{r}\frac{\partial w}{\partial r}+\frac{1}{r^2}\frac{\partial^2 w}{\partial \theta^2}\right)^2 + 2D_{r\theta}\left(\frac{\partial}{\partial r}\left(\frac{1}{r}\frac{\partial w}{\partial \theta}\right)\right)^2\right] r\,dr\,d\theta$$

$$T=\frac{h}{2}\int_0^{2\pi}\int_{R_{inner}}^{R_{outer}}\left[\sigma_{rr}\left(\frac{\partial w}{\partial r}\right)^2+\sigma_{\theta\theta}\left(\frac{1}{r}\frac{\partial w}{\partial \theta}\right)^2\right] r\,dr\,d\theta \tag{2}$$

where D_r, D_θ, $D_{r\theta}$ and D_1 are the bending rigidities as defined in the notation.

Thus, equilibrium configurations corresponding to nontrivial values of the transverse displacement $w(r,\theta)$ are obtained by enforcing the stationarity of the total potential energy, U:

$$\partial U=\partial(V+T)=0 \tag{3}$$

In applying the Rayleigh–Ritz method, the out of plane displacement $w(r,\theta)$ is expressed as:

$$w(r,\theta)=\sum_{n=1}^{N_{Ritz}} A_n\phi_n(r)\cos(\lambda\theta) \tag{4}$$

where

$$\phi_n(r)=r^{n-1}\left(1-\frac{r}{R_{outer}}\right)^2 \tag{5}$$

$\phi_n(r)(n=1,2,3)$ are three kinematically admissible shape functions of r and the terms A_n are arbitrary coefficients to be determined from the stationary condition (3). Starting with one term (i.e. $n=1$), the approximation of $w(r,\theta)$ was systematically improved up to $n=3$, as convergence to the critical load with three terms was found to be adequate. For the isotropic degenerate case $w(r,\theta)$ is approximated as $w(r,\theta)=A(1-(r/R_{outer})^2)^2\cos(\lambda\theta)$ which is a one term aproximating function similar to that used in Ref. 12.

Upon substituting (4) into (2) for V and T, we arrive at the following result:

$$V=\sum_{m=1}^{3}\sum_{n=1}^{3} V_{mn}A_mA_n$$

$$T=\sum_{m=1}^{3}\sum_{n=1}^{3} T_{mn}A_mA_n \tag{6}$$

where

$$V_{mn}=\frac{\pi}{2}\int_{R_{inner}}^{R_{outer}}\left[D_r\phi_m''\phi_n''+2D_1\phi_m''\left(\frac{1}{r}\phi_n'-\frac{\lambda^2}{r^2}\phi_n\right) + D_\theta\left(\frac{1}{r}\phi_m'-\frac{\lambda^2}{r^2}\phi_m\right)\left(\frac{1}{r}\phi_n'-\frac{\lambda^2}{r^2}\phi_n\right) + 2D_{r\theta}\lambda^2\left(\frac{\phi_m'}{r}\right)\left(\frac{\phi_n'}{r}\right)\right] r\,dr$$

$$T_{mn}=\pi h\int_{R_{inner}}^{R_{outer}}\left[\sigma_{rr}\phi_m'\phi_n'+\sigma_{\theta\theta}\frac{\lambda^2}{r^2}\phi_m\phi_n\right] r\,dr \tag{7}$$

Thus it follows from (3) that,

$$\frac{\partial(V+T)}{\partial A_m}=\sum_{n=1}^{3}(V_{mn}+V_{nm}+T_{mn}+T_{nm})A_n=0 \tag{8}$$

where T_{mn} is linear in the bifurcation load. Using (7) in (8), we obtain the three bifurcation loads, of which the lowest is our critical buckling load. The solution of the resulting equations will be discussed in a later section.

2.2 Rectilinearly orthotropic annulus

The problem formulation for the rectilinearly orthotropic annulus is complicated by the fact that the lay-up of the material is rectilinear while the geometry of the annulus is polar. Because of this, there exists no exact solution to the pre-buckling stresses and an approximate pre-buckling stress state is calculated utilizing Galerkin's method. The buckling solution is similar to the analyses for the polar orthotropic annulus and is performed with the Rayleigh–Ritz method.

The problem configuration for the rectilinearly orthotropic annulus subjected to uniform internal or external pressure is as shown in Fig. 1b. In this figure, q is the uniformly distributed axisymmetric external pressure loading and p is the uniformly

distributed axisymmetric internal pressure loading. In the present analyses, we are only considering a single ply of rectilinearly orthotropic composite. Thus our annulus is generally orthotropic in the x-y plane. The formulation that follows can be utilized for any number of plies as long as the laminate lay-up is symmetric about the mid-plane.

The governing equations for the prebuckling stress state are:

$$\begin{aligned}(rN^0_{rr})_{,r}+N^0_{r\theta,\theta}-N^0_{\theta\theta}&=0\\ N^0_{\theta\theta,\theta}+(rN^0_{r,\theta})_{,\theta}+N^0_{r\theta}&=0\end{aligned} \tag{9}$$

where N^0_{rr}, $N^0_{\theta\theta}$ and $N^0_{r\theta}$ are the pre-buckling, thickness averaged, stress resultants. In the pre-buckled state, the strain-displacement relations are,

$$\begin{aligned}\varepsilon^0_{rr}&=u_{,r}\\ \varepsilon^0_{\theta\theta}&=\frac{v_{,r}}{r}+\frac{u}{r}\\ \varepsilon^0_{r\theta}&=v_{,r}+\frac{u_{,\theta}}{r}-\frac{v}{r}\end{aligned} \tag{10}$$

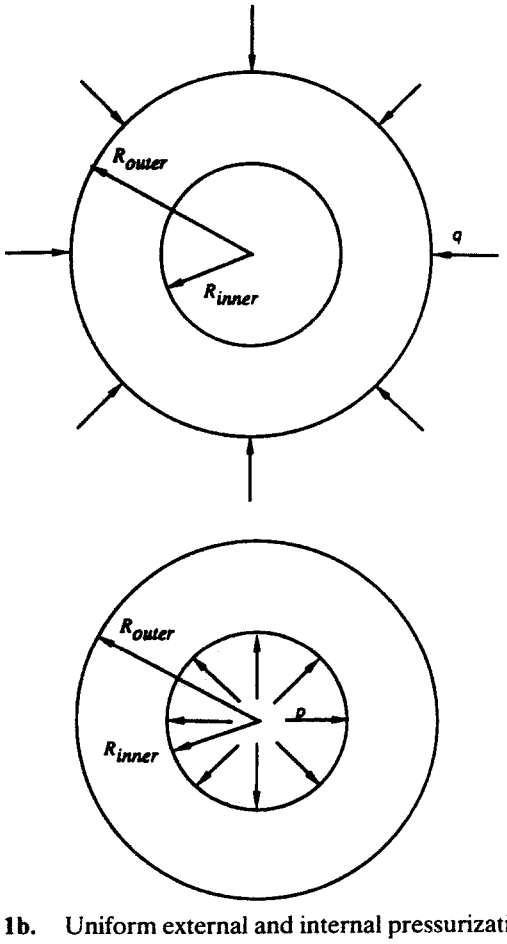

Fig. 1b. Uniform external and internal pressurization.

where u and v are the in-plane deformations in the radial and circumferential directions respectively. From Classical Lamination Theory one knows that,

$$\begin{Bmatrix}N^0_{rr}\\ N^0_{\theta\theta}\\ N^0_{r\theta}\end{Bmatrix}=\begin{bmatrix}A_{11}(\theta) & A_{12}(\theta) & A_{16}(\theta)\\ A_{12}(\theta) & A_{22}(\theta) & A_{26}(\theta)\\ A_{16}(\theta) & A_{26}(\theta) & A_{66}(\theta)\end{bmatrix}\begin{Bmatrix}\varepsilon^0_{rr}\\ \varepsilon^0_{\theta\theta}\\ \varepsilon^0_{r\theta}\end{Bmatrix} \tag{11}$$

The reduced stiffnesses, $\bar{Q}_{ij}$, for any one ply, needed to define $A_{ij}(\theta)$ in (11) are given by,

$$\begin{aligned}\bar{Q}_{11}&=Q_{11}\cos^4(\alpha)+2(Q_{12}+2Q_{66})\\ &\quad\times\cos^2(\alpha)\sin^2(\alpha)+Q_{22}\sin^4(\alpha)\\ \bar{Q}_{12}&=(Q_{11}+Q_{22}-4Q_{66})\sin^2(\alpha)\cos^2(\alpha)\\ &\quad+Q_{12}(\sin^4(\alpha)+\cos^4(\alpha))\\ \bar{Q}_{16}&=(Q_{11}-Q_{12}-2Q_{66})\sin(\alpha)\cos^3(\alpha)\\ &\quad+(Q_{12}-Q_{22}+2Q_{66})\sin^3(\alpha)\cos(\alpha)\\ \bar{Q}_{22}&=Q_{11}\sin^4(\alpha)+2(Q_{12}+2Q_{66})\\ &\quad\times\sin^2(\alpha)\cos^2(\alpha)+Q_{22}\cos^4(\alpha)\\ \bar{Q}_{26}&=(Q_{11}-Q_{12}-2Q_{66})\sin^3(\alpha)\cos(\alpha)\\ &\quad+(Q_{12}-Q_{22}+2Q_{66})\sin(\alpha)\cos^3(\alpha)\\ \bar{Q}_{66}&=(Q_{11}+Q_{22}-2Q_{12}-2Q_{66})\sin^2(\alpha)\cos^2(\alpha)\\ &\quad+Q_{66}(\sin^4(\alpha)+\cos^4(\alpha))\end{aligned} \tag{12}$$

where Q_{ij} is the stiffness matrix of a single ply and α is the angle which describes the orientation between the material axis and the principal axis of the ply. Various types of anisotropy are discussed in Ref. 11.

Since the annulus is analysed with reference to a polar coordinate system, we need to transform the $[\bar{Q}_{ij}]$ matrix which is in the x-y coordinate system into $[\hat{Q}_{ij}]$, which describes the material properties of the composite in the r-θ coordinate system as follows,

$$[\hat{Q}_{ij}]=[T_\sigma][\bar{Q}_{ij}][T_\sigma]^{\text{Transpose}} \tag{13}$$

where

$$[T_\sigma]=\begin{bmatrix}\cos^2(\theta) & \sin^2(\theta) & 2\sin(\theta)\cos(\theta)\\ \sin^2(\theta) & \cos^2(\theta) & -2\sin(\theta)\cos(\theta)\\ -\sin(\theta)\cos(\theta) & \sin(\theta)\cos(\theta) & \cos^2(\theta)-\sin^2(\theta)\end{bmatrix} \tag{14}$$

Thus, the $[A_{ij}(\theta)]$ matrix for a n-ply symmetric laminate is given by,

$$A_{ij} = \sum_{k=1}^{N} \int_{h_{k-1}}^{h_k} \hat{Q}_{ij}^{(k)} \, dz \tag{15}$$

where in general the A_{ij} terms are θ dependent.

The force approach is used to determine the pre-buckling stress distribution. This is accomplished by the introduction of the Airy stress function which satisfies the equilibrium equations (9) exactly. Thus, the relationship between the Airy stress function, Φ, and the pre-buckling stress resultants is given by,

$$\begin{aligned} N_{rr}^0 &= \frac{\Phi_{,r}}{r} + \frac{\Phi_{,\theta\theta}}{r^2} \\ N_{\theta\theta}^0 &= \Phi_{,rr} \\ N_{r\theta}^0 &= -\left(\frac{\Phi_{,\theta}}{r}\right)_{,r} \end{aligned} \tag{16}$$

The governing equation for Φ is obtained via the compatibility equation,

$$\varepsilon_{rr,\theta\theta}^0 - r\varepsilon_{rr,r}^0 + r(r\varepsilon_{\theta\theta}^0)_{,r\theta} = 0 \tag{17}$$

Substitution of the pre-buckling stress resultants into (17) above and utilizing (11), we obtain the following equation,

$$\begin{aligned} &a_{22} r^4 \Phi_{,rrrr} + (2a_{22} - a_{26,\theta}) r^3 \Phi_{,rrr} - 2a_{26} r^3 \Phi_{,rrr\theta} \\ &+ (a_{12,\theta\theta} - a_{26,\theta} - a_{16,\theta} - a_{11}) r^2 \Phi_{,rr} \\ &+ (2a_{12} + a_{66}) r^2 \Phi_{,rr\theta\theta} + (2a_{12,\theta} + a_{66,\theta}) r^2 \Phi_{,rr\theta} \\ &+ (a_{11} + a_{11,\theta\theta}) r \Phi_{,r} + (2a_{11,\theta} - a_{16,\theta\theta} \\ &- 2a_{16} - 2a_{26} - a_{66,\theta\theta}) r \Phi_{,r\theta} \\ &+ (-2a_{12} - a_{66} - 3a_{16,\theta}) r \Phi_{,r\theta\theta} - 2a_{16} r \Phi_{,r\theta\theta\theta} \\ &+ (2a_{16} + 2a_{26} + a_{66,\theta} + a_{16,\theta\theta}) \Phi_{,\theta} \\ &+ (2a_{11} + 2a_{12} + a_{66} + 3a_{16,\theta} + a_{11,\theta\theta}) \Phi_{,\theta\theta} \\ &+ (2a_{16} + 2a_{11,\theta}) \Phi_{,\theta\theta\theta} + a_{11} \Phi_{,\theta\theta\theta\theta} = L_F \Phi = 0 \end{aligned} \tag{18}$$

where $L_F\Phi$ is the differential operator of the equation and $[a_{ij}] = [A_{ij}]^{-1}$.

In utilizing the Galerkin method we assume

$$\Phi(r, \theta) = \Phi_o(r, \theta) + \sum_{n=1}^{N_{Gal}} a_n \Phi_n(r, \theta) \tag{19}$$

$\Phi_0(r, \theta)$ is chosen in (19) such that it satisfies the boundary conditions. That is, the stresses due to $\Phi_n(r, \theta)$ must vanish at the boundary. The unknown coefficients, a_n, are evaluated through the Galerkin procedure as follows,

$$\int_A [L_F \Phi(r, \theta)] \, \Phi_m \, dA = 0 \tag{20}$$

Thus we obtain,

$$\int_A \left[\left[L_F \Phi_o(r, \theta) + \sum_{n=1}^{N_{Gal}} a_n L_F \Phi_n(r, \theta) \right] \Phi_m(r, \theta) \right] \times dA = 0 \tag{21}$$

which implies,

$$\int_A L_F \Phi_p(r, \theta) \, \Phi_m(r, \theta) \, dA + \sum_{n=1}^{N_{Gal}} a_n \int_A L_F \Phi_n(r, \theta) \, \Phi_m(r, \theta) \, dA = 0 \tag{22}$$

Re-arranging (22) into matrix form to solve for the unknown coefficients, a_n, we obtain,

$$[K_{ij}]\{a_j\} = \{P_i\} \tag{23}$$

where

$$\begin{aligned} K_{mn} &= \int_A L_F \Phi_n(r, \theta) \, \Phi_m(r, \theta) \, dA \\ P_m &= \int_A L_F \Phi_o(r, \theta) \, \Phi_m(r, \theta) \, dA \end{aligned} \tag{24}$$

The above set of linear eqns (23) are solved to obtain the unknown coefficients, a_n, from which the Airy stress function is obtained. Once the Airy stress function is calculated, the pre-buckling stress resultants are computed through eqn (16).

Since we have a generally orthotropic annulus, the potential energy V, due to the pre-buckling stresses, and the work done by the external forces, T, are given by,

$$\begin{aligned} V &= \frac{1}{2} \int_A \int_{h_{n-1}}^{h_n} [\sigma_{rr}\varepsilon_{rr} + \sigma_{\theta\theta}\varepsilon_{\theta\theta} + \sigma_{r\theta}\varepsilon_{r\theta}] \, dz \, dA \\ T &= \frac{1}{2} \int_A [N_{rr}^0 \varepsilon_{rr}^0 + N_{\theta\theta}^0 \varepsilon_{\theta\theta}^0 + N_{r\theta}^0 \varepsilon_{r\theta}^0] \, dA \end{aligned} \tag{25}$$

thus we have,

$$V=\frac{1}{2}\int_A [D_{11}(\theta)\kappa_{rr}^2+D_{22}(\theta)\kappa_{\theta\theta}^2+D_{66}(\theta)\kappa_{r\theta}^2 + 2D_{12}(\theta)\kappa_{rr}\kappa_{\theta\theta}+2D_{16}(\theta)\kappa_{rr}\kappa_{r\theta} + 2D_{26}(\theta)\kappa_{\theta\theta}\kappa_{r\theta}]\, r\,dr\,d\theta$$

$$T=\frac{1}{2}\int_A [N_{rr}^0\varepsilon_{rr}^0+N_{\theta\theta}^0\varepsilon_{\theta\theta}^0+N_{r\theta}^0\varepsilon_{r\theta}^0]\, r\,dr\,d\theta \quad (26)$$

where the flexural rigidities D_{ij} for a n-ply laminate are defined as follows:

$$D_{ij}=\sum_{n=1}^{N}\hat{Q}_{ij}^n(\theta)(h_n^3-h_{n-1}^3) \quad (27)$$

The curvatures, κ_{rr}, $\kappa_{\theta\theta}$ and $\kappa_{r\theta}$, and the strains, ε_{rr}, $\varepsilon_{\theta\theta}$ and $\varepsilon_{r\theta}$, are defined to be

$$\varepsilon_{rr}=\frac{1}{2}w_{,r}^2;\quad \varepsilon_{\theta\theta}=\frac{1}{2r^2}w_{,\theta}^2;\quad \varepsilon_{r\theta}=\frac{1}{r}w_{,r}w_{,\theta} \quad (28)$$

$$\kappa_{rr}=-w_{,rr};\quad \kappa_{\theta\theta}=-\left[\frac{1}{r}w_{,r}+\frac{1}{r^2}w_{,\theta\theta}\right];$$

$$\kappa_{r\theta}=-2\left[\frac{1}{r}w_{,r\theta}-\frac{1}{r^2}w_{,\theta}\right]$$

Utilizing the Rayleigh–Ritz method, the out of plane displacement, $w(r,\theta)$, is approximated by,

$$w(r,\theta)=\sum_{n=1}^{N_{\text{Ritz}}}A_n\phi_n(r)\cos(\lambda\theta) \quad (29)$$

where N_{Ritz} is the total number of Rayleigh–Ritz terms taken in the approximation. The total potential of the annulus at buckling, U, is given by $U=V+T$ and from the stationary condition, $\delta(U)=0$, we obtain the critical buckling load. Substituting (29) into (26) and taking the variation of U we have,

$$V=\sum_{m=1}^{N_{\text{Ritz}}}\sum_{n=1}^{N_{\text{Ritz}}}V_{mn}A_mA_n$$

$$T=\sum_{m=1}^{N_{\text{Ritz}}}\sum_{n=1}^{N_{\text{Ritz}}}T_{mn}A_mA_n \quad (30)$$

$$\delta(U)=\delta(V+T)=\frac{\partial(V+T)}{\partial A_m}$$

Equation (30) yields N_{Ritz} linear homogeneous simultaneous equations in the arbitrary parameters as given below

$$\sum_{n=1}^{N_{\text{Ritz}}}(V_{mn}+V_{nm}+T_{mn}+T_{nm})A_n=\sum_{n=1}^{N_{\text{Ritz}}}I_{mn}A_n=0 \quad (31)$$

where V_{mn} is given by,

$$V_{mn}=\frac{1}{2}\int_0^{2\pi}\int_{R_{\text{inner}}}^{R_{\text{outer}}}\left\{\left[D_{11}(\theta)\phi_{m,rr}\phi_{n,rr} + D_{22}(\theta)\left(\frac{\phi_{m,r}}{r}-\frac{\lambda^2}{r^2}\phi_m\right)\left(\frac{\phi_{n,r}}{r}-\frac{\lambda^2}{r^2}\phi_n\right) + 2D_{12}(\theta)\phi_{m,rr}\left(\frac{\phi_{n,r}}{r}-\frac{\lambda^2}{r^2}\phi_n\right)\right]\cos^2(\lambda\theta) + \left[4D_{16}(\theta)\phi_{m,rr}\left(\frac{\lambda}{r}\phi_{n,r}-\frac{\lambda^2}{r^2}\phi_n\right) + 4D_{26}(\theta)\left(\frac{\phi_{m,r}}{r}-\frac{\lambda^2}{r^2}\phi_m\right) \times\left(\frac{\lambda}{r}\phi_{n,r}-\frac{\lambda^2}{r^2}\phi_n\right)\right]\sin(\lambda\theta)\cos(\lambda\theta) + 4D_{66}(\theta)\left(\frac{\lambda}{r}\phi_{m,r}-\frac{\lambda^2}{r^2}\phi_m\right) \times\left(\frac{\lambda}{r}\phi_{n,r}-\frac{\lambda^2}{r^2}\phi_n\right)\sin^2(\lambda\theta)\right\} r\,dr\,d\theta \quad (32)$$

and T_{mn} by,

$$T_{mn}=\frac{1}{2}\int_0^{2\pi}\int_{R_{\text{inner}}}^{R_{\text{outer}}}\left\{N_{rr}^0\phi_{m,r}\phi_{n,r}\cos^2(\lambda\theta) + N_{\theta\theta}^0\frac{\lambda^2}{r^2}\phi_m\phi_n\sin^2(\lambda\theta) - N_{r\theta}^0\frac{\lambda}{r}\phi_{m,r}\phi_n\sin(\lambda\theta)\cos(\lambda\theta)\right\} r\,dr\,d\theta \quad (33)$$

The T_{mn} term is linear in p, the external uniform pressure, or q, the internal uniform pressure. Nontrivial solutions of eqn (31) are obtained by setting the determinant associated with eqn

(31) to zero. The lowest load associated with this condition is identified as the critical buckling load. It is found that the rectilinear orthotropic formulation for a specially orthotropic composite reduces to the polar orthotropic formulation if the following substitutions are made.

$$D_r=\frac{E_r h^3}{12(1-\nu_r\nu_\theta)}$$

$$D_\theta=\frac{E_\theta h^3}{12(1-\nu_r\nu_\theta)} \tag{34}$$

$$D_{r\theta}=\frac{G_{r\theta}h^3}{12}$$

$$D_1=\nu_r D_\theta$$

where the elastic moduli E_r, E_θ, $G_{r\theta}$ and ν_r are related to the elastic moduli of the generally rectilinearly orthotropic composite by

$$E_r=\left(\frac{1}{E_1}\cos^4(\theta)+\left(\frac{1}{G_{12}}-\frac{2\nu_{12}}{E_1}\right)\sin^2(\theta)\cos^2(\theta)+\frac{1}{E_2}\sin^4(\theta)\right)^{-1}$$

$$E_\theta=\left(\frac{1}{E_1}\sin^4(\theta)+\left(\frac{1}{G_{12}}-\frac{2\nu_{12}}{E_1}\right)\sin^2(\theta)\cos^2(\theta)+\frac{1}{E_2}\cos^4(\theta)\right)^{-1} \tag{35}$$

$$G_{r\theta}=\left(2\left(\frac{2}{E_1}+\frac{2}{E_2}+\frac{4\nu_{12}}{E_1}-\frac{1}{G_{12}}\right)\sin^2(\theta)\cos^2(\theta)+\frac{1}{G_{12}}(\sin^4(\theta)+\cos^4(\theta))\right)^{-1}$$

$$\mu_r=E_r\left(\frac{\nu_{12}}{E_1}(\sin^4(\theta)+\cos^4(\theta))-\left(\frac{1}{E_1}+\frac{1}{E_2}-\frac{1}{G_{12}}\right)\sin^2(\theta)\cos^2(\theta)\right)$$

where E_1, E_2 and G_{12} are the Young's moduli and shear moduli of the orthotropic annuli in the principal material axes, and ν_{12}, ν_{21} are Poisson's ratios.

3 SOLUTION PROCEDURE

Numerical work was carried out in both the polar orthotropic and the rectilinearly orthotropic cases by utilizing the symbolic manipulation programs Mathematica and Reduce. The calculations were compared to those obtained by using a Fortran program. The symbolic manipulation packages were found to be efficient and to yield superior accuracy. The procedure to obtain the buckling loads were as follows. For a given annulus geometry and for a fixed number of Ritz terms in the radial direction, the buckling loads obtained from the determinant condition were examined as a function of λ. A minimum buckling load was identified, corresponding to a specific value of λ. This procedure was continued by increasing the number of Ritz terms in the radial direction and checking for convergence.

For both load cases, as shown in Fig. 1b, the buckling analysis is performed with the outer edge simply supported and the inner edge free. Thus, the plate kinematic boundary conditions at the outer edge are:

$$w(R_{\text{outer}},\theta)=0,\ \frac{\partial w}{\partial r}(R_{\text{outer}},\theta)=0 \tag{36}$$

The orthotropic material constants used are listed in Table 1.

4 RESULTS AND DISCUSSION

In the isotropic case, our formulation produces results which agree with those reported in Refs 12–14.

Table 1. Orthotropic material properties used in the numerical calculations

	D_r (N m)	D_θ (N m)	$D_{r\theta}$ (N m)	D_1 (N m)	h (m)
Fig. 2a	7·6046	7·6046	2·5095	2·5095	1·04E-3
Fig. 2b	1·118E4	0·625E4	0·533E3	0·335E4	0·01
Fig. 3a	1·118E4	0·625E4	0·533E3	0·335E4	0·01
Fig. 3b	0·625E4	1·118E4	0·533E3	0·335E4	0·01
Fig. 4a	1·118E4	0·625E4	0·533E3	0·335E4	0·01
Fig. 4b	0·625E4	1·118E4	0·533E3	0·335E4	0·01

	E_1 (N m^2)	E_2 (N m^2)	G_{12} (N m^2)	ν_{12}	h (m)
Fig. 5a	111E9	13E9	6·4E9	0·38	0·01
Fig. 5b	111E9	13E9	6·4E9	0·38	0·01

For this case, material properties corresponding to aluminium were used in conjunction with the following one term Rayleigh-Ritz approximating shape function,

$$w(r,\theta)=A\left(1-\left(\frac{r}{R_{\text{outer}}}\right)^2\right)^2\cos(\lambda\theta) \qquad (37)$$

where A is an unknown constant. This shape function is the same as that used in Ref. 12. However, in Ref. 12 the axisymmetric ($\lambda=0$) case was obtained analytically and the nonaxisymmetric ($\lambda>0$) cases were obtained using the Rayleigh-Ritz method while in our analysis, all the results ($\lambda=0$ and $\lambda>0$ cases) were obtained numerically from the degenerative orthotropic formulation. The general topology of the results shown in Fig. 2a agree well with those in Ref. 12.

4.1 Polar orthotropic annulus

Results obtained for polar orthotropic ($k=0{\cdot}747$) material properties and external uniform pressure loading, using 1, 2 and 3 Ritz approximating terms from eqns (3) and (4) are shown in Fig. 2b. The curves demonstrate the convergence characteristics of the solution process. It is noted that the process of adding terms can be continued indefinitely lending to a lowering of the buckling load. The lowest value for the buckling load is obtained when the approximation to $w(r,\theta)$ corresponds to the exact analytic solution. However, adding an additional term to the two-term approximation only lowers the buckling load slightly, and for our required degree of accuracy of four significant figures in the buckling load, a three-term approximation was found to be sufficient. Thus in the remainder of the polar orthotropic analysis, all computation performed with the Rayleigh-Ritz approximation utilized only three kinematically admissible approximating terms. In each case convergence was checked and found to be adequate.

For the polar orthotropic ($k=0{\cdot}747$), and externally pressurized case, it is observed (refer to Fig. 3a) that for $\lambda=0$, the shape of the buckling curve is similar to $\lambda=0$ for the isotropic case. This is so because for axisymmetric buckling, the buckling load is only affected by the variables in the axisymmetric direction.

For $\lambda>0$, there exist values of λ which produce buckling loads lower than the corresponding axisymmetric buckling values. Thus, an axisymmetric buckling mode assumption in the formulation leads to a buckling load that is not minimized.

It is also found from Fig. 3a that for aspect ratios close to unity, approximating a ring, the buckling load is lower than for aspect ratios close to zero, approximating a plate. This can be attributed to the ease in buckling a narrow annulus nonaxisymmetrically, somewhat analogous to an axially compressed narrow and long plate that develops several waves lengthwise at buckling.

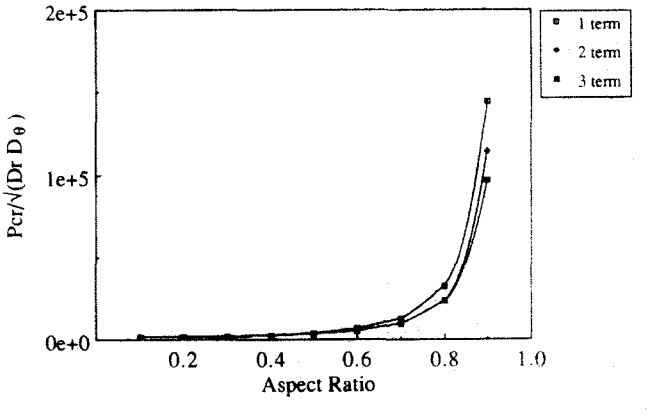

Fig. 2b. Rate of convergence, for the polar orthotropic, $k=0{\cdot}747$, externally pressurized case.

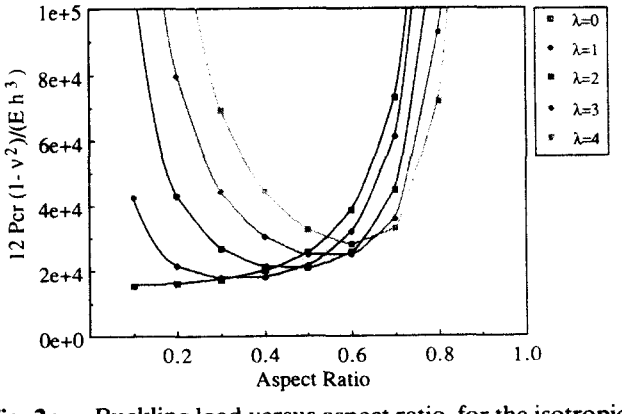

Fig. 2a. Buckling load versus aspect ratio, for the isotropic, externally pressurized case.

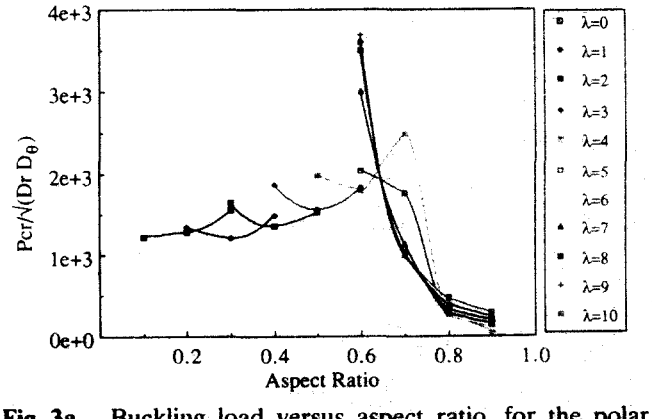

Fig. 3a. Buckling load versus aspect ratio, for the polar orthotropic, $k=0{\cdot}747$, externally pressurized case.

We find, for nonaxisymmetric buckling, a peak in the buckling load at an aspect ratio of approximately 0·7. This can be attributed to the trade-off between axisymmetric and nonaxisymmetric buckling as the geometry of the plate approaches that of a ring. In other words, the ability to sustain an axisymmetric buckling mode decreases for increasing aspect ratios, due to the decrease in effective width $R_{outer} - R_{inner}$ of the annulus while a nonaxisymmetric buckling mode is favoured for increasing aspect ratio.

In Fig. 3b we present results for $k = 1{\cdot}34$, with uniform external pressurization. In this case the radial modulus is lower than the circumferential modulus by the definition of k. This would dictate that the annulus would be stiffer in the circumferential as opposed to the radial direction, thereby causing the annulus to go into nonaxisymmetric buckling at a higher aspect ratio than for $k < 1$. Comparison of Fig. 3b with Fig. 3a confirms the above observation, as the first appearance of a nonaxisymmetric buckling load is at a higher aspect ratio for $k = 1{\cdot}34$ than for $k = 0{\cdot}747$. Further, nonaxisymmetric buckling in this case prevails for a wide range of aspect ratios as shown in Fig. 3b. Therefore, assumptions of axisymmetric buckling here again produces erroneous buckling loads that are not minimized.

In the cases where the annulus is internally pressurized, we see from eqn (2) that the prebuckling membrane stress component $\sigma_{\theta\theta}$ is negative, thereby inferring tensile loads. This would tend to preclude nonaxisymmetric buckling modes. This is confirmed by our results in Fig. 4a ($k = 0{\cdot}747$) and Fig. 4b ($k = 1{\cdot}34$). Comparing the results in Figs 4a and 4b, we see that the critical buckling load corresponding to $k = 1{\cdot}34$ is higher than that corresponding to $k = 0{\cdot}747$. Again this is to be expected because for $k > 1$, the circumferential modulus is greater than the radial modulus; thus an internal uniform pressure will tend to stiffen the annulus and cause the axisymmetric buckling load to increase. This situation is analogous to a square plate with compressive forces in one axis direction and tensile forces in the other; the buckling load of a similar plate under compression in both directions, will have a lower buckling load.

4.2 Rectilinearly orthotropic annulus

The formulation for the rectilinearly orthotropic annulus reduces to that of the polar orthotropic annulus when appropriate simplifications are carried out as shown by eqns (34) and (35). Thus, the results for the polar orthotropic and isotropic annuli can be obtained from the rectilinearly orthotropic formulation. For this case, the prebuckling stress distribution was obtained via a Galerkin approximation with 15 approximating functions. The stress distribution obtained from such a numerical calculation was checked by

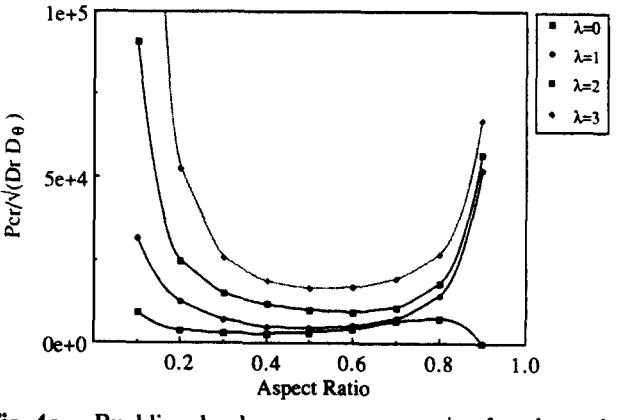

Fig. 4a. Buckling load versus aspect ratio, for the polar orthotropic, $k = 0{\cdot}747$, internally pressurized case.

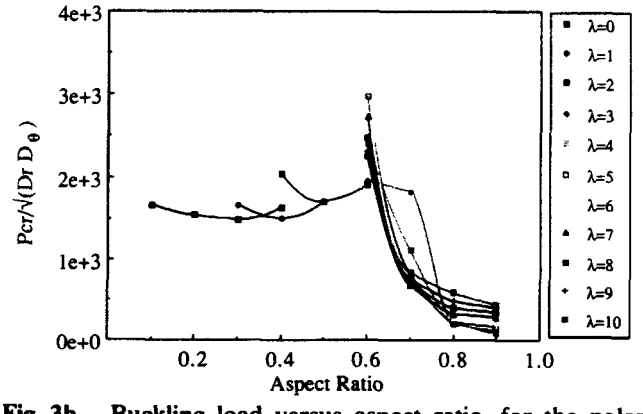

Fig. 3b. Buckling load versus aspect ratio, for the polar orthotropic, $k = 1{\cdot}34$, externally pressurized case.

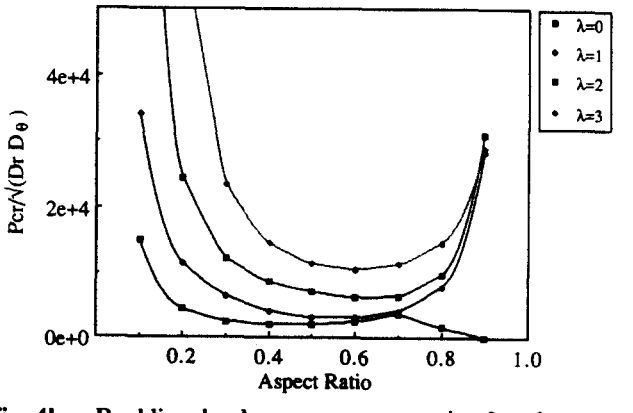

Fig. 4b. Buckling load versus aspect ratio, for the polar orthotropic, $k = 1{\cdot}34$, internally pressurized case.

'cutting' the annulus diametrically and checking equilibrium. A 15 term Galerkin approximation to the pre-buckling stresses was found to be more than adequate.

The buckling analysis was performed by using the pre-buckling stress approximation obtained via the Galerkin method and a Rayleigh–Ritz procedure. A four-term Rayleigh–Ritz approximation in the radial direction was found to be adequate here.

Results obtained for the rectilinearly orthotropic and externally pressurized case are similar to those obtained for the corresponding case of a polar orthotropic annulus in that the lowest buckling load is associated predominantly with nonaxisymmetric buckling. This is expected since the buckling mode is more sensitive to the geometry (aspect ratio) of the annulus and the applied loading than to the material properties. From Fig. 5a we can see that axisymmetric buckling modes exist for aspect ratios up to 0·5 after which nonaxisymmetric buckling prevails. It is also shown in Fig. 5a that as the aspect ratio increases, the buckling loads corresponding to various modes associated with nonaxisymmetric buckling become closer and closer showing that the buckling load is independent of the circumferential mode number. It is also found in the rectilinearly orthotropic case that the nonaxisymmetric buckling load associated with high aspect ratios (0·8 and 0·9) is smaller than that for low aspect ratios. This is due to the fact that at high aspect ratios the annulus approximates a ring and the circumferential stiffness is low resulting in lower nonaxisymmetric buckling loads.

From the pre-buckling analysis, it is found that $\sigma^0_{r\theta}$ is non-zero for both the rectilinearly orthotropic cases. For the case of uniform external pressure, the predominant mode associated with the minimum buckling load is found not to be affected by a nonzero $\sigma^0_{r\theta}$. This is also found to be true for the internally pressurized case. A nonzero $\sigma^0_{r\theta}$ is found not to be significant enough to force the internally pressurized rectilinearly orthotropic annulus to buckle nonaxisymmetrically. As is demonstrated in Fig. 5b, the buckling mode for the range of aspect ratios studied is axisymmetric, just as in the corresponding case for the polar orthotropic annulus. It can also be seen in this figure that the buckling loads at all aspect ratios for different buckling modes are very close to each other, showing that any imperfection in the annulus may strongly influence the buckling mode.

5 CONCLUSION

Buckling of polar orthotropic and rectilinearly orthotropic annular plates subjected to uniform in-plane radial edge pressures have been analysed herein for fixed outer edge, free inner edge boundary conditions. In the analysis, the Rayleigh–Ritz method was employed with simple polynomials in r coupled with a trigonometric cosine term as admissible functions to describe both the axisymmetric and nonaxisymmetric modes of buckling. The pre-buckling stress resultants used in the buckling analysis for the polar orthotropic cases were exact and are obtained from Ref. 8 while the pre-buckling stress resultants for the rectilinearly orthotropic cases were obtained approximately with Galerkin's method.

It is demonstrated for both polar and rectilinearly orthotropic annuli with external radial loading that over a wide range of aspect ratios, the dominant buckling mode is nonaxisymmetric. If assumptions of axisymmetry are enforced, the

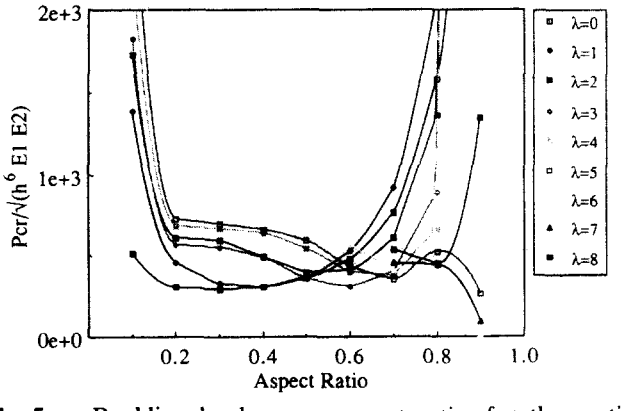

Fig. 5a. Buckling load versus aspect ratio, for the rectilinearly orthotropic, externally pressurized case.

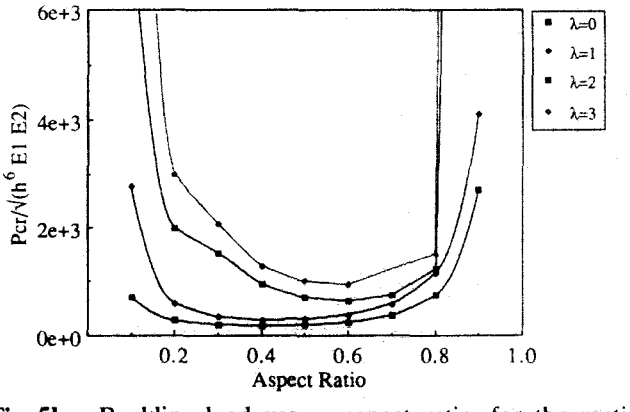

Fig. 5b. Buckling load versus aspect ratio, for the rectilinearly orthotropic, internally pressurized case.

buckling loads thus obtained will not be minimized. In contrast, it is found that in the corresponding internally pressurized cases, the dominant buckling mode is axisymmetric.

The buckling mode is found to be highly dependent on the aspect and rigidity ratios of the annulus. Bimodal buckling is observed at certain aspect ratios, including the isotropic case, showing that the critical buckling load can be related to two different modes. At high aspect ratios for the externally loaded cases, it is found that multimodal buckling can occur as the buckling loads for the different modes are very close to each other, and whether the annulus buckles into one mode shape or the other will then be controlled by any initial imperfection of the annulus. This same conclusion holds true for all aspect ratios in the internally pressurized cases. Also we find that as the annulus becomes narrower, it prefers to buckle with a higher wave number, λ, and a lower buckling load, analogous to the case of an axially compressed long and narrow plate.

It is also noted that our results for the annulus at high aspect ratios ($> 0{\cdot}8$) may not be the actual buckling loads. This is because at high aspect ratios, in-plane buckling effects come into play and the lowest buckling load may now be associated with an in-plane buckling mode.

ACKNOWLEDGEMENTS

The authors acknowledge the financial support received from the Rackham Graduate School at the University of Michigan. The authors are appreciative of the support and help from Mr Amir Khamseh during the initial phase of this work.

REFERENCES

1. Pandalai, K. A. V. & Patel, S. A., Buckling of orthotropic circular plates. *Journal of the Royal Aeronautical Society*, **69** (1965) 279–80.
2. Woinowsky-Krieger, S. M., Buckling stability of circular plates with circular cylindrical aelotropy. *Ingenieur-Archiv*, **26** (1958) 129–31.
3. Ramaiah, G. K. & Vijayakumar, K., Buckling of polar orthotropic annular plates under uniform internal pressure. *AIAA Journal*, **12** (8) (August 1974) 1045–50.
4. Uthegenannt, E. B. & Brand, B. S., Buckling of orthotropic annular plates. *AIAA Journal*, **8** (11) (1970) 2102–4.
5. Cheng Chang-Jin, Duan Wei & Parker, D. F., Elastic instability of polar orthotropic annular plates. *International Journal of Engineering Science*, **27** (2) (1989) 109–21.
6. Huang, C. L., Post buckling of an annulus. *AIAA Journal*, **11** (12) (December 1972) 1608–12.
7. Mossakowski, J., Buckling of circular plates with cylindrical orthotropy. *Archiwum Mechaniki Stosowanej*, **12** (1960) 583–96.
8 Lekhnitsky, S. G., *Anisotropic Plates*, 1st edn (English trans.) (contributions to the Metallurgy of Steel No. 50). American Iron and Steel Institute, New York, 1956, p. 77.
9. Simitses, G. J. & Frostig, Y., Radially compressed laminated circular plates. *Composite Structures*, **9** (1988) 1–17.
10 Vijayakumar, K. & Joga Rao, C. V., Buckling of polar orthotropic annular plates. *Transactions of the ASCE, Journal of Engineering Mechanics Division*, **97** (EM3) (June 1971) 701–10.
11. Whitney, J., *Structural Analysis of Laminated Anisotropic Plates*. Technomic Publishing, Stamford, CN, 1987.
12. Majumdar, S., Buckling of a thin annular plate under uniform compression. *AIAA Journal*, **9** (9) (September 1971) 1701–7.
13. Yamaki, N., Buckling of a thin annular plate under uniform compression. *Report of the Institute of High Speed Mechanics, Sendai, Japan*, **10** (1959) 129–47.
14. Dean, W. R., The elastic stability of an annular plate. *Proceedings of the Royal Society of London, Ser. A*, **106** (1924) 268–84.